JOURNAL OF THERMOPHYSICS AND HEAT TRANSFER
Vol. 24, No. 3, July–September 2010

Influence of Compressibility on Film-Cooling Performance

Kiran H. Dellimore,* André W. Marshall,† and Christopher P. Cadou†
University of Maryland, College Park, Maryland 20742

DOI: 10.2514/1.45092

Film-cooling is an active cooling technique that is widely used in conventional gas turbine and rocket engines to manage heat transfer between hot reacting gases and cooler structural components. It is also a candidate technology for the thermal protection of scramjet engines, in which combustion occurs under highly compressible conditions. This paper extends semi-empirical modeling ideas for incompressible wall-jet slot film-cooling to account for both convective and thermal compressibility effects. The new model shows that the influence of compressibility is determined by the magnitude of the average convective Mach number M_c, the total temperature ratio $\theta_0 = T_{0s}/T_{0\infty}$, and the flow Mach number M_{HS} of the highest-speed stream in the film-cooling flow. In general, increasing M_c and decreasing θ_0 improves film-cooling performance. These predictions are validated via comparison with experimental data in three compressible flow regimes: weakly compressible (M_c, $M_{\mathrm{HS}} \leq 0.3$ and $0.6 \leq \theta_0 \leq 1$), moderately compressible ($0.3 < M_c, M_{\mathrm{HS}} \leq 1.0$, and $0.30 \leq \theta_0 < 0.60$), and highly compressible ($M_c, M_{\mathrm{HS}} > 1.0$, and $\theta_0 < 0.3$). The model also resolves disagreements in the literature over the importance of compressibility in film-cooling problems by showing that compressibility effects can be significant, provided the convective and flow Mach numbers are high enough and the total temperature ratio is low enough.

Nomenclature

A_0, A_1, A_2	=	integration constants
a	=	speed of sound
b	=	shear-layer (wall-jet) thickness
b_0	=	film-cooling louver thickness
C'_{M_0}	=	turbulent mixing coefficient
c	=	ratio of density in mixing zone I at the transition point to the coolant-stream density
$\mathrm{d}b/\mathrm{d}x$	=	unnormalized shear-layer growth rate
d_0, E_0, K	=	empirical constants
I_v	=	average transverse turbulence intensity
M	=	Mach number
M_c	=	convective Mach number
m	=	mass
R	=	ratio of the average hot-stream velocity to the average coolant-stream velocity, U_∞/U_s
S	=	density ratio, ρ_s/ρ_∞
s	=	louver slot height
T	=	absolute temperature
U	=	average fluid stream velocity
x	=	streamwise distance
x_0	=	streamwise location of the point of coolant injection
x_1	=	streamwise location of the transition point between the initial and fully developed regions
y	=	transverse distance
y_1	=	transverse location of the shear-layer/coolant-stream interface
y_2	=	transverse location of the shear-layer/hot-stream interface
α	=	ratio of specific heats parameter
γ	=	ratio of specific heats
δ'	=	normalized shear-layer growth rate
η_{eff}	=	compressible film-cooling effectiveness, $(T_{0\infty} - T_{0\mathrm{aw}})/(T_{0\infty} - T_{0s})$
θ	=	dimensionless static temperature ratio
θ_0	=	dimensionless ratio of coolant to mainstream total temperature
λ	=	blowing ratio, $\rho_s U_s/\rho_\infty U_\infty$
μ	=	dynamic viscosity
ξ	=	similarity parameter
ρ	=	fluid density
σ	=	dimensionless flow-temperature grouping
χ	=	compressible initial region factor
ψ	=	dimensionless temperature ratio
ω	=	dimensionless flow-temperature grouping

Subscripts

aw	=	adiabatic wall
c	=	characteristic or convective
comp	=	compressible
HS	=	high speed
i	=	initial
r	=	recovery
s	=	coolant stream
0	=	stagnation conditions
I	=	zone I of shear layer
II	=	zone II of shear layer
∞	=	hot-gas stream

Presented as Paper 2008-5032 at the 44th AIAA/ASME/SAE/ASEE Joint Propulsion Conference and Exhibit, Hartford CT, 21–23 July 2008; received 22 April 2009; accepted for publication 23 January 2010.

*Graduate Student, Department of Aerospace Engineering. Student Member AIAA.

†Associate Professor, Department of Aerospace Engineering. Senior Member AIAA.

I. Introduction

FILM-COOLING is an active cooling strategy involving the continuous injection of a thin layer of fluid near a wall to provide thermal protection from a hot-gas flow. It is widely used in gas turbine engines to protect turbine blades and combustor liners and in rocket motors, in which it is used to protect thrust-chamber walls and nozzle extensions. Film-cooling is also a candidate technology for thermal protection in supersonic combustion ramjet (scramjet) engines. However, achieving efficient film-cooling is extremely challenging because of the inherently complex geometric and fluid dynamic environment present in many gas turbine and rocket engines [1]. The large velocities and temperature differences present in these systems suggest that compressibility could have an important influence on film-cooling effectiveness. Therefore, the objective of

the current study is to investigate the influence of compressibility on film-cooling performance.

Over the past 50 years, many experimental, numerical, and theoretical studies of film-cooling performance under compressible conditions have been conducted [2–15]. However, the results of these studies are often contradictory and a consensus regarding the importance of compressibility has not emerged. For example, Volchkov et al. [2] performed a theoretical investigation of the effect of velocity and temperature compressibility on film-cooling effectiveness by deriving a film-cooling correlation based on an energy and momentum analysis of a boundary layer. They compared their results with experimental data from Durgin [3] for the film-cooling of a cone at Mach 3.5 and concluded that compressibility effects are very small and to first order can be ignored in practical calculations. This conclusion was corroborated by the theoretical work of Repukhov [4], who transformed the turbulent-boundary-layer equations to account for the effects of compressibility and nonisothermal conditions on film-cooling performance. He compared his theoretical predictions with experimental data for the tangential-slot film-cooling of a flat plate at a coolant injection Mach number of 0.4. Repukhov found that compressibility effects can be ignored over a wide range of velocity and temperature conditions. In contrast, experimental work by Hansmann et al. [5] suggests that compressibility can significantly influence film-cooling performance. Their investigation of tangential-slot film-cooling of a flat plate in a high-enthalpy wind tunnel (2000 K < T < 3000 K, 0.5 < M < 1.0, air and helium working fluids) showed that film-cooling performance strongly depended on the density and velocity ratios (coolant to mainstream), with higher effectiveness observed as the velocity and density ratios were increased. Similar results have also been reported by Pedersen et al. [6], who investigated the effects of large density differences between the mainstream and coolant stream on the cooling performance of three-dimensional hole injection over a flat plate. Their results showed that increasing the density ratio (by mixing various amounts of helium, carbon dioxide, refrigerant F-12, and air into the main and film streams) increases the cooling efficiency. Pedersen et al. also noted that this effect was most pronounced at large blowing ratios ($M > 1$), where increases in effectiveness of greater than 200% were observed.

The present study attempts to sort out these discrepancies by extending Simon's [16] semi-empirical incompressible film-cooling analysis to account for the effects of velocity and temperature compressibility. The predictions of the resulting compressible film-cooling model (CFM) are evaluated by comparing them with experimental film-cooling data [14,17,18] in three distinct compressibility regimes: weak, moderate, and strong. This is followed by an explanation and discussion of velocity and temperature compressibility effects on film-cooling based on the predictions of the CFM. Conclusions are then drawn regarding the overall influence of compressibility on film-cooling performance.

II. Analysis

Figure 1 is a schematic illustration of the wall-jet film-cooling model proposed by Simon [16]. The figure shows a coolant stream at a temperature T_{0s} and Mach number M_s being injected near the wall from a slot of height s. At x_0, the coolant stream encounters a hot-gas stream of temperature $T_{0\infty}$ (with $T_{0\infty} > T_{0s}$), moving at a velocity M_∞, where $M_\infty < M_s$. A weakly turbulent shear layer of thickness b develops and grows with streamwise distance x at the interface between the coolant and hot-gas streams. The length of the initial developing region x_1 is taken to be the distance required for the inner edge of the developing mixing zone, labeled zone I in Fig. 1, to reach the wall. This region is often called the potential core and the region upstream of its impingement point has been shown to provide very effective protection [19].

Following the approach of Simon [16], the adiabatic wall temperature in the initial region ($x < x_1$), T_{aw}, is assumed to equal the mean fluid total temperature in zone II (coolant zone) in the developing region the adiabatic wall temperature is assumed to equal the mean fluid total temperature in zone I. Hence,

$$T_{\text{aw}} = \begin{cases} \bar{T}_{0\text{II}}, & (x < x_1) \\ \bar{T}_{0\text{I}}, & (x \geq x_1) \end{cases} \tag{1}$$

The following assumptions are also made:

1) The change in the specific heat with temperature is small.
2) The hot-gas-stream temperature, T_∞, is constant.
3) Thermal radiation from the hot-gas stream is negligible.
4) The shear-layer growth b is linear.
5) No pressure gradient is present.

Under compressible conditions, the film-cooling effectiveness is typically defined in terms of the recovery temperature [20]:

$$\eta_{\text{eff}} = \frac{T_{r\infty} - T_{\text{aw}}}{T_{r\infty} - T_{rs}} \tag{2}$$

Since the recovery temperature is usually very close to the stagnation temperature, it is common practice to approximate the effectiveness as [21]

$$\eta_{\text{eff}} \approx \frac{T_{0\infty} - T_{\text{aw}}}{T_{0\infty} - T_{0s}} \tag{3}$$

Performing a mass and energy balance on the coolant stream shown in Fig. 1, following Stollery and El-Ehwany [22], shows that the film-cooling effectiveness is related to the amount of hot-stream gas entrained by the coolant stream:

$$\eta_{\text{eff}} = \frac{\dot{m}_s}{\dot{m}_f} \tag{4}$$

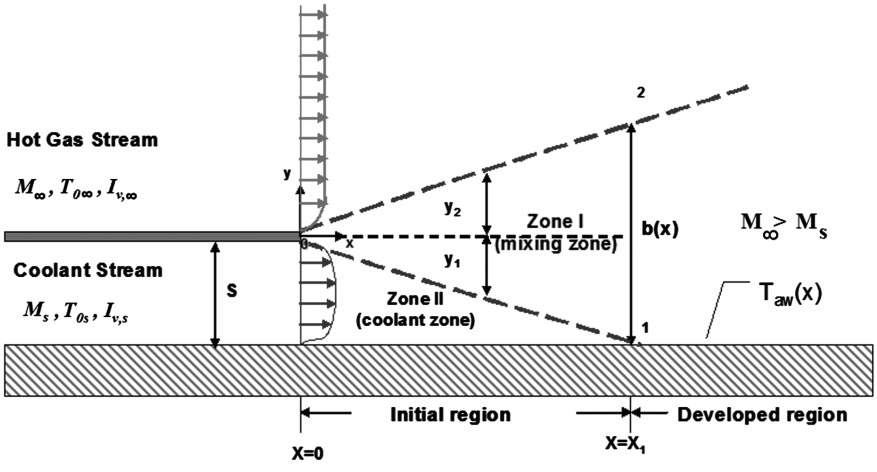

Fig. 1 Wall-jet film-cooling model adapted from Simon [16].

In this expression, $\dot{m}_s$ is the coolant mass flow rate per unit length, $\dot{m}_s = \rho_s U_s s$, and $\dot{m}_f$ is the total mass flow rate of the film per unit length at any arbitrary x location downstream of the coolant slot exit. Note that $\dot{m}_f$ is the sum of both the coolant mass flow rate per unit length and the entrained hot-gas stream rate per unit length $\dot{m}'_e$:

$$\dot{m}_f = \dot{m}_s + \int_0^x \dot{m}'_e \, \mathrm{d}x \tag{5}$$

Following Juhasz and Marek [23], $\dot{m}'_e$ is assumed to be directly proportional to the hot-gas-stream mass flux:

$$\dot{m}'_e = C'_{M_0} \rho_\infty a_\infty M_\infty \tag{6}$$

where C'_{M_0} is an effective turbulent mixing coefficient, which is a function of the average flowfield turbulence intensity I_v.

Substitution of Eqs. (5) and the definition of $\dot{m}_s$ into Eq. (4) yields the correlation

$$\eta_{\text{eff}} = [1 + (x/\lambda s) C'_{M_0}]^{-1} \tag{7}$$

where λ is the blowing ratio, which is defined as the ratio of the coolant-stream to hot-stream mass flux:

$$\lambda = \rho_s M_s a_s / \rho_\infty M_\infty a_\infty \tag{8}$$

Equation (7) gives the functional form for a basic turbulent film-cooling correlation. It shows that film-cooling effectiveness decreases with increasing streamwise distance, with decreasing blowing ratio, with decreasing slot height, and with increasing turbulence intensity.

The turbulent mixing coefficient C'_{M_0} is defined following Simon's [16] approach in terms of a turbulent mixing coefficient C_{M_0} and a turbulent diffusion parameter χ :

$$C'_{M_0} = \frac{C_{M_0} - \chi (x/\lambda s)^{-1}}{1 + \chi} \tag{9}$$

The parameter χ in Eq. (9) accounts for turbulent diffusion from zone I to zone II in the initial region ($x < x_1$) only and $\chi = 0$ in the developed region ($x \geq x_1$). The turbulent diffusion parameter is given by

$$\chi = \{C_{M_0}(x/\lambda s) + (x/x_1) - E_0 I^*_{v,s} (T_{0s}/T_{0\text{aw}_{x=x_1}}) \times Ln[1/(1 - x/x_1)]\} \left(\frac{T_{\text{aw}_{x=x_1}} - T_{\text{aw}}}{T_{0\infty} - T_{0s}} \right) \tag{10}$$

where E_0 is an empirically determined constant.

Continuing in an analogous manner to Simon [16], we find an expression for C'_{M_0} in terms of C_{M_0} and χ by assuming that C_{M_0} is a function of the shear-layer entrainment rate $\mathrm{d}b/\mathrm{d}x$. This growth rate can be directly related to I_v by using Abramovich's [24] empirical assumption that $\mathrm{d}b/\mathrm{d}x$ is proportional to the perturbation component of the fluctuating hot-gas-stream velocity v'_i. This leads to

$$C_{M_0} = \mathrm{d}b/\mathrm{d}x = \frac{d_0 v'_i}{u_c} \tag{11}$$

where d_0 is an empirical constant and u_c is the characteristic velocity of the shear layer given by

$$u_c = \int_{y2}^{y1} \rho u \, \mathrm{d}y \Big/ \int_{y2}^{y1} \rho \, \mathrm{d}y \tag{12}$$

An approximate expression for u_c can be obtained by using a weighted average between the two streams as proposed by Yakovlevskiy [25]:

$$u_c = \frac{\rho_\infty a_\infty M_\infty + \rho_s a_s M_s}{\rho_\infty + \rho_s} \tag{13}$$

Substituting Eq. (13) into Eq. (11), simplifying by noting that $I_v = v'_i / M_\infty a_\infty$, and incorporating Eq. (8) yields an expression for C_{M_0}, which, can be written as

$$C_{M_0} = d_0 (I_v \sigma)^K \tag{14}$$

In this expression, K is an empirically determined constant, σ is a dimensionless flow-temperature parameter developed by Simon [16], and I_v is the overall average transverse turbulence intensity; σ and I_v are given by

$$\sigma = (1 + 1/\theta)/(1 + \lambda) \tag{15}$$

$$I_v = I_{v,\infty} + 0.4(|I_{v,\infty} - I_{v,s}|) \tag{16}$$

where θ is the temperature ratio, which is defined as the ratio of the coolant to hot-stream static temperature T_s/T_∞. $I_{v,s}$ is the initial average transverse coolant-stream turbulence intensity, and $I_{v,\infty}$ is the initial average transverse turbulence intensity of the hot-gas stream. I_v is based on a turbulent correlation obtained from Ko and Liu [26], which has the constraint that I_v cannot be greater than either $I_{v,\infty}$ or $I_{v,s}$.

The final step in the development of a useful compressible film-cooling model is determining the location of the transition point between the initial and fully developed regions, x_1, that appears in Eq. (10). This is typically referred to as the impingement or persistence length. From the geometry of the shear layer in Fig. 1,

$$x_1 = x(s/y_1) \tag{17}$$

where y_1 is the shear-layer/coolant-stream interface position.

Since the shear-layer thickness is given by $b = y_1 + y_2$, and the turbulent mixing coefficient C_{M_0} is related to the shear-layer growth rate by $C_{M_0} = (b - y_1)/x$, Eq. (17) can be rewritten as

$$x_1 = [(C_{M_0}/s)(y_1/y_2)]^{-1} \tag{18}$$

Abramovich's [24] semi-empirical theory of turbulent compressible shear layers is used to determine y_1/y_2 in Eq. (18). Abramovich showed that the growth rate $\mathrm{d}b/\mathrm{d}x$ for a compressible shear layer formed between two coflowing streams at different Mach numbers is given by

$$\mathrm{d}b/\mathrm{d}x = \pm c/2(1 - R)(1 + \bar{S})/(1 + R\bar{S}) \tag{19}$$

where R is the ratio of the average hot-stream velocity to the average coolant-stream velocity (i.e., $R = M_\infty a_\infty / M_s a_s$), and c is a growth-rate constant, which is a function of the density ratio between the two streams. The negative sign is taken when $R > 1$ and corresponds to a core-driven film. S is the ratio of the average hot-stream to coolant-stream density, $\bar{S} = \rho_\infty / \rho_s$. It can be expressed in terms of the coolant injection Mach number referenced at sonic conditions [27] M^*_s as

$$\bar{S} = \frac{\sigma \theta_0 (1 - \alpha_s M^{*2}_s)}{(1 - \alpha_s M^{*2}_s \theta_0 \Omega \sigma R^2)} \tag{20}$$

Here, θ_0 is the coolant to hot-stream total temperature ratio ($\theta_0 = T_{0s}/T_{0\infty}$), $\alpha_s = \gamma_s - 1/\gamma_s + 1$, and $\Omega = [(\gamma_\infty - 1)/(\gamma_s + 1)](\gamma_s/\gamma_\infty)$, and σ is the ratio of molecular weights of the two streams ($\sigma = \mathrm{MW}_\infty/\mathrm{MW}_s$).

Substituting Eq. (20) into Eq. (19) yields the following expression for the shear-layer growth rate:

$$\mathrm{d}b/\mathrm{d}x = \pm c/2(1 - R) \frac{(1 - \alpha_s M^{*2}_s \theta_0 \Omega \sigma R^2) + \sigma \theta_0 (1 - \alpha_s M^{*2}_s)}{(1 - \alpha_s M^{*2}_s \theta_0 \Omega \sigma R^2) + \sigma \theta_0 R (1 - \alpha_s M^{*2}_s)} \tag{21}$$

Equation (21) shows that the growth in the compressible shear-layer thickness is solely a function of the velocity ratio, total temperature ratio, and chemical composition of the two mixing streams and that

the shear-layer thickness varies linearly with streamwise distance. Integrating Eq. (21) and performing a mass and momentum balance on the two streams gives an expression for y_1/b. Abramovich [24] did this for the case when $\theta_0 = 1$ and both streams are of identical chemical composition yielding the following result:

$$y_1/b = A_0 - 2A_1 + A_2 + R(A_1 - A_2) \tag{22}$$

The parameters A_0, A_1, and A_2 in Eq. (22) are defined in terms of dimensionless density and velocity ratios $\rho/\rho_s(\xi)$ and $U/U_s(\xi)$:

$$A_0 = \int_0^1 \rho(\xi)/\rho_s \, \mathrm{d}\xi \tag{23}$$

$$A_1 = \int_0^1 \rho(\xi)/\rho_s U(\xi)/U_s \, \mathrm{d}\xi \tag{24}$$

$$A_2 = \int_0^1 \rho(\xi)/\rho_s (U(\xi)/U_s)^2 \, \mathrm{d}\xi \tag{25}$$

Abramovich [24] assumed that the velocity and temperature (density) profiles across the shear layer are universal and can be expressed in terms of a similarity parameter ξ, given by

$$\xi = (y - y_2)/b \tag{26}$$

The functional forms for both the velocity and temperature profiles through the shear layer were selected based on empirical measurements. Schlichting's [28] law of 3/2 was assumed for the velocity profile, whereas a linear distribution was assumed for the temperature profile, based on an empirical formulation by Zhestkov (as reported by Abramovich [23]). These assumptions led to the following expressions for the variation of the velocity and density through the layer in terms of the similarity coordinate:

$$U(\xi)/U_s = (1 - \xi^{3/2})^2 \tag{27}$$

$$\frac{\rho}{\rho_s}(\xi) = \frac{1 - \alpha_s M_s^{*2}}{1 - \alpha_s M_s^{*2}[1 - U(\xi)/U_s(\xi)(1 - R)]^2} \tag{28}$$

In the problem of interest here, where the total temperature and chemical composition also vary through the layer, an analogous analysis shows that Eq. (28) should be replaced by

$$\frac{\rho}{\rho_s} = \frac{\sigma(\xi)\theta_0}{[1 + (\theta_0 - 1)\xi]} \left\{ \frac{1 - \alpha_s M_s^{*2}}{1 - \Omega(\xi)\sigma(\xi)\theta_0 \alpha_s M_s^{*2} \frac{[1 - U(\xi)/U_s(\xi)(1-R)]^2}{1 + (\theta_0 - 1)\xi}} \right\} \tag{29}$$

where $\Omega(\xi) = (\gamma(\xi) - 1/\gamma_s + 1)(\gamma_s/\gamma(\xi))$, and $\sigma(\xi) = \mathrm{MW}(\xi)/\mathrm{MW}_s$.

Assuming that the composition, like the temperature, also varies linearly through the layer [i.e., $\Omega(\xi)$ and $\sigma(\xi)$ are linear functions of ξ] leads to the following expression for the density ratio:

$$\frac{\rho}{\rho_s} = \frac{[1 + \varphi(\xi)]\theta_0}{[1 + (\theta_0 - 1)\xi]} \times \left\{ \frac{1 - \alpha_s M_s^{*2}}{1 - \left[\frac{1 - 1/\gamma_s + \psi(\xi)}{1 + \psi(\xi)}\right][1 + \varphi(\xi)]\theta_0 \alpha_s M_s^{*2} \frac{[1 - U(\xi)/U_s(\xi)(1-R)]^2}{1 + (\theta_0 - 1)\xi}} \right\} \tag{30}$$

where $\varphi(\xi) = (\xi - 1)(1 - \mathrm{MW}_\infty/\mathrm{MW}_s)$ and $\psi(\xi) = (\xi - 1)(1 - \gamma_\infty/\gamma_s)$. Equations (30) and (27) are substituted into Eqs. (23–25) but does not yield an expression that can be integrated analytically. Therefore, a numerical approach will be explained in the next section. Once A_0, A_1, and A are found, Eq. (22) is rearranged to obtain an expression for y_1/y_2 [recall that $b = y_1 + y_2$ (see Fig. 1)]:

$$y_1/y_2 = \{-1 + 1/c[A_0 - 2A_1 + A_2 + R(A_1 - A_2)]\}^{-1} \tag{31}$$

As in Simon [16], c is defined to be a function of the fluid density ratio in mixing zone I at the impingement point. Since the pressure is constant across the layer and the chemical composition is assumed to be uniform, the density ratio is given by

$$c = (T_{0s}/T_{\mathrm{aw}_{x=x1}})\left(1 + \frac{\gamma - 1}{2} M_s^2\right)^{-1} \tag{32}$$

Equations (31) and (32), combined with Eqs. (7–10), and (18) form a CFM that is valid for both homogeneous and heterogeneous wall-jet film-cooling in the absence of a pressure gradient under compressible flow conditions.

III. Numerical Integration Procedure

The integrals in Eqs. (23–25) are approximated using an N-point Gauss–Legendre quadrature rule [29]:

$$\int_0^1 f(x) \, \mathrm{d}x = \frac{1}{2} \sum_{i=1}^{N} w_i f\left(\frac{1}{2} x_i + \frac{1}{2}\right) + R_n \tag{33}$$

where $f(x)$ is the function being integrated, x_i are the ith roots of orthogonal Legendre polynomials $P_n(x)$, w_i are the weights for $i = 1, \ldots, N$ such that $w_i = 2/[(1 - x_i)^2 (P_n'(x_i))^2]$ and R_n is the residual. Here, $P_n'(x_i)$ is the derivative of the Legendre polynomial with respect to x. This quadrature method was selected because it is typically more accurate than other methods for the same number of function evaluations and because it converges quickly [30].

Figure 2 shows the residuals associated with A_0, A_1, and A_2 as a function of the number of points used to make the approximation for the $M_c = 0.30$ test case explored by Ferri et al. [14]. The residual is estimated following Stoer and Bulirsch [30] as the difference between the approximation to the integral at a given order n and the approximation at the order $n - 1$. In this work, n is chosen to ensure that the residual associated with each parameter is always less than 1.0×10^{-6}. The figure shows that 11 points are sufficient to ensure convergence for this test case.

IV. Data Sources for Model Parameters

To preserve the analogy to the incompressible model, the values of the empirical parameters d_0, E_0, K, $I_{v,s}$, and $I_{v,\infty}$, are assumed to be independent of compressibility. Therefore, they can be inferred by performing a least-squares analysis to find the values that produce the best fit to experimental data. This least-squares approach has been employed successfully in previous work [31]. Data from three film-cooling studies were used to select values for d_0, E_0, and K. These studies were selected because they reported turbulence intensity

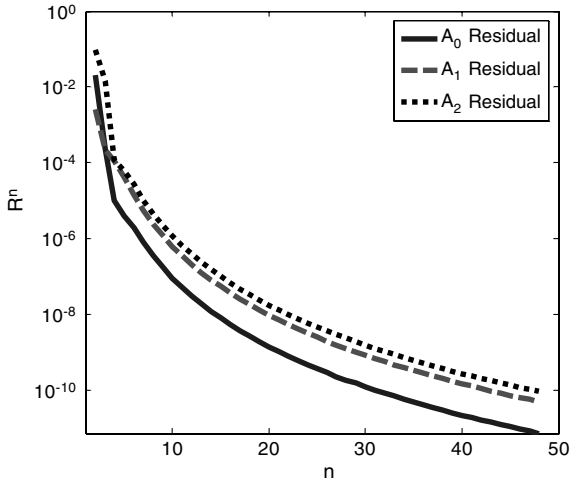

Fig. 2 Residual R_n as a function of the number of points n associated with the Gauss–Legendre quadrature of A_0, A_1, and A_2 for the $M_c = 0.30$ case of Ferri et al. [14].

Table 1 Summary of experimental conditions from various film-cooling studies [14,17,18] used to validate the CFM

Study	λ	M_s	M_∞	M_c	θ_0	R	S	s, m	$I_{v,s}$, %	$I_{v,\infty}$, %	d_0	E_0	K
Ferri et al. [14]	0.50	0.32	0.80	0.30	0.58	3.13	1.57	9.0×10^{-4}	3.0	3.0	0.015	13.7	0.28
Cary and Hefner [17]	0.08	1.00	6.00	1.29	0.62	2.91	0.24	11.1×10^{-3}	2.0	2.0	0.65	13.7	0.177
Cruz et al. [18]	2.22	0.09	0.05	0.015	0.71	0.64	1.41	4.2×10^{-3}	5.0	1.6	0.495	13.7	0.859

measurements and covered a broad range of compressible conditions. Brief explanations of the data and summaries of our findings (see Table 1) are presented below.

Ferri et al. [14] studied tangential-slot film-cooling in a turbulent boundary layer using an axisymmetric subsonic wind tunnel. Tests were performed at three different mainstream Mach numbers: 0.8, 0.6, and 0.4. The total temperature of the main flow was 500 K. Coolant air was injected over a range of Mach numbers from 0.1 to 1, at a total temperature of 289 K. Blowing ratios between 0.5 and 1.7 were attained and the average mainstream turbulence intensity, $I_{v,\infty}$, was measured to be 3.0%. Since no measurement for the average coolant-stream turbulence intensity $I_{v,s}$ is reported, it assumed that $I_{v,s}$ and $I_{v,\infty}$ are equal. A sensitivity analysis was performed to determine the influence of the empirical parameters E_0, K, and d_0. This analysis showed that the compressible film-cooling model is insensitive to the value of E_o, so it was simply set to the value used by Simon [16] of 13.7. The remaining model parameters K and d_o were found using a two-variable least-squares analysis to be 0.00653 and 0.080, respectively.

Cary and Hefner [17] reported equilibrium temperature and skin friction measurements at the surface of a flat plate in a Mach 6 airstream cooled by sonic, tangential-slot injection. Tests were conducted with a mainstream total temperature of 478 K, coolant total temperatures between 166 and 311 K, and three different coolant injection-slot heights: 1.58, 4.78, and 11.1 mm. The average coolant-stream and hot-stream turbulence intensities $I_{v,s}$ and $I_{v,\infty}$ were not reported; however, these values were estimated previously by Luschik et al. [32] using numerical simulations at identical conditions. Luschik et al. found that setting $I_{v,s}$ and $I_{v,\infty}$ to approximately 2%, yielded numerical predictions that agreed well with the experimental results. A least-squares analysis shows that choosing K equal to 0.0254 and d_o equal to 0.155 produces the best fit between the model and the experimental results.

Cruz et al. [18] reported film-cooling effectiveness as a function of downstream distance x in a subsonic hot-wind-tunnel facility. The mainstream velocity and temperature were 20.0 m/s and 431 K, respectively. The velocity and temperature of the coolant stream were 31.5 m/s and 306 K. Laser Doppler velocimetry measurements indicated that the average coolant-stream turbulence intensity $I_{v,s}$ was 5.0%, and the average hot-stream turbulence intensity $I_{v,\infty}$ was 1.6%. Previous work [31] showed that choosing K equal to 0.8592 and d_o equal to 0.4950 produced the best correspondence between the model and the experimental data.

V. Results

A. Quantifying Compressibility Effects

Before examining some of the results obtained from the compressible film-cooling model, it is useful to present and discuss three parameters that are commonly used to quantify compressibility effects. The first is the average convective Mach number M_c first proposed by Papamoschou et al. [33–35] as a means to correlate compressibility effects in mixing-layer flows (of which film-cooling flows are a subset). It is defined as the speed at which a disturbance propagates in a mixing layer relative to the speed of sound [34] and can be written as follows:

$$M_c = \frac{U_\infty - U_s}{a_\infty + a_s} \tag{34}$$

where a_∞ and a_s are the mainstream and coolant-stream speeds of sound, respectively. Mixing layers with convective Mach numbers less than 0.3 are effectively incompressible.

The second is the total temperature ratio $\theta_0 = T_{0s}/T_{0\infty}$, which was suggested by Abramovich [24] as a means of quantifying thermal compressibility in mixing layers. Flows with total temperature ratios near unity exhibit weak thermal compressibility, whereas flows with total temperature ratios far from unity exhibit strong thermal compressibility. Only studies in which $\theta_0 \leq 1$ are considered here since hot-gas-stream total temperatures are always equal to or greater than coolant-stream total temperatures in practical film-cooling applications.

The third parameter is the Mach number, M_{HS}, of the highest-speed stream in the film-cooling flow. In practice, this is usually the mainstream Mach number, but in some cases it can be the coolant-stream Mach number.

B. Compressibility Regimes

We can identify three distinct compressibility regimes in film-cooling flows based on the values of the compressibility parameters defined above. The weak regime corresponds to low convective and flow Mach numbers M_c and $M_{\mathrm{HS}} \leq 0.3$ as well as near-unity total temperature ratios: approximately in the range $0.6 \leq \theta_0 \leq 1$. In this regime, velocity and thermal compressibility effects are generally very small to negligible and the flow is essentially incompressible. The moderate regime corresponds to convective and flow Mach numbers roughly in the range of $0.3 < M_c$, $M_{\mathrm{HS}} \leq 1$ and total temperature ratios in the range of $0.30 \leq \theta_0 < 0.60$. Here, the effects of thermal and velocity compressibility are present and become more pronounced with increasing convective Mach number and decreasing total temperature ratio. The strong compressibility regime corresponds to convective and flow Mach numbers greater than unity, i.e., $M_C, M_{\mathrm{HS}} > 1$, and to total temperature ratios less than 0.3, i.e., $\theta_0 < 0.3$. In this regime, compressibility effects are expected to be significant.

In the following subsections, we explore the effects of compressibility on film-cooling performance in each regime by comparing the model's prediction of the downstream variation of effectiveness to those of Simon's incompressible model (SM) [16] and various experimental measurements. The values of the model parameters used in each case are summarized in Table 1. A detailed summary of Simon's incompressible film-cooling model has been presented in previous work [31].

1. *Weak Compressibility Regime*

Figure 3 shows film-cooling effectiveness as a function of nondimensional streamwise distance for a turbulent weakly compressible wall jet, where $\theta_0 = 0.71$, $M_c = 0.015$, and $M = 0.09$. The mainstream Mach number in this case is 0.05, the coolant-stream Mach number is 0.09, and the slot height is 4.2 mm. The x symbols correspond to experimental data from Cruz et al. [18], the solid line corresponds to the predictions of the SM, and the dashed line corresponds to the CFM predictions under identical conditions. The figure shows that under weakly compressible conditions, the predictions of the CFM, agree to within an average difference of 0.3% with those of the SM. This makes sense, because the CFM $\rightarrow$ SM in the limit that $M_c, M \rightarrow 0$, since from Eq. (20) $T_0 \rightarrow T$. The CFM model also matches measurements by Cruz et al. [18] to within a maximum difference of 11.4%. The small difference between the SM and CFM curves in the near-injection region ($x/\lambda s < 40$) is due to the fact that the total temperature ratio is less than unity and therefore that there is a very weak thermal compressibility effect present. This causes a slight reduction in the growth of the shear layer at the coolant/mainstream interface, which pushes the impingement point further downstream, thereby leading the CFM to predict a

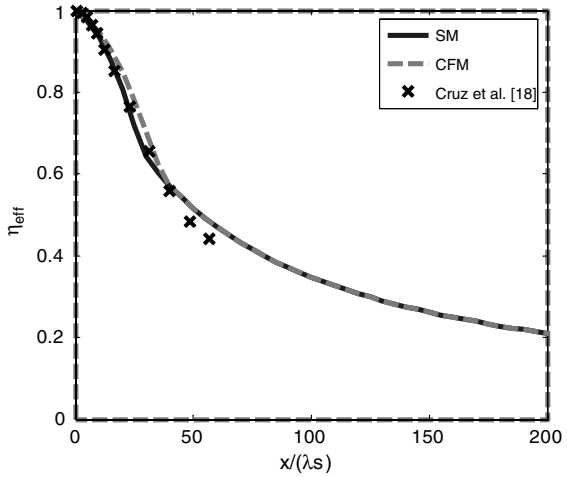

Fig. 3 Plot of film-cooling efficiency η_{eff} as a function of nondimensional streamwise distance $x/(\lambda s)$ for a turbulent wall jet at $\theta_0 = 0.71$ and $M_c = 0.015$ as predicted by the CFM and the SM.

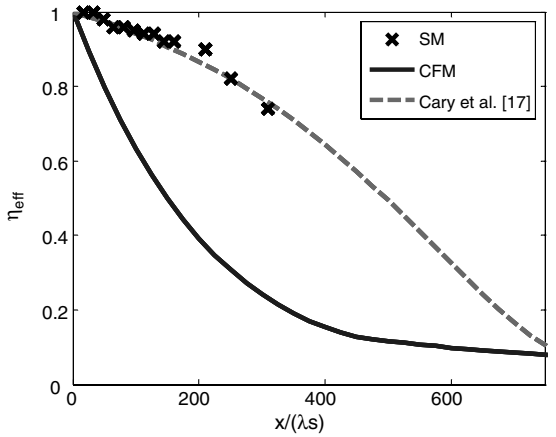

Fig. 5 Plot of film-cooling efficiency η_{eff} as a function of nondimensional streamwise distance $x/(\lambda s)$ for a turbulent core-driven film at $\theta_0 = 0.62$ and $M_c = 1.29$ as predicted by the CFM and the SM.

slightly higher effectiveness than the SM. Beyond the impingement point, the film mixes rapidly, driving the total temperature ratio to 1 and thereby eliminating the difference between the SM and CFM in the far-field region ($x/\lambda s > 40$).

2. Moderate Compressibility Regime

Figure 4 shows the variation of film-cooling effectiveness with nondimensional streamwise distance for a turbulent weakly compressible wall jet, where $\theta_0 = 0.58$, $M_c = 0.31$, and $M = 0.80$. The coolant-stream Mach number is 0.32, and the slot height is 0.89 mm. The x symbols correspond to experimental data from Ferri et al. [14], the solid lines correspond to the predictions of the SM, and the dashed lines correspond to the CFM predictions under identical conditions. The figure shows that the CFM correlates the experimental measurements much better than the SM; the average difference between the CFM and experiment in the near-slot region ($x/(\lambda s) < 75$) is 3.0%, compared with nearly 10% for the SM. The significant improvement in correlation to experimental data demonstrates the importance of compressibility on film-cooling performance.

3. Strong Compressibility Regime

Figure 5 shows film-cooling effectiveness as a function of nondimensional streamwise distance for a turbulent highly compressible wall jet with $\theta_0 = 0.62$, $M_c = 1.29$, and $M = 6.00$. Experimental data from Cary and Hefner [17] is shown using x symbols, while the solid lines and dashed lines correspond to the predictions of the SM and the CFM, respectively. The figure highlights the importance of incorporating compressibility effects when convective Mach numbers are high and temperature ratios deviate significantly from unity. The average difference between the CFM and experimental data is 1.8%, whereas the SM fails completely. Taken together, the results from Secs. V.B.1, V.B.2, and V.B.3 indicate that compressibility can have important and, in some cases, dramatic effects on film-cooling performance.

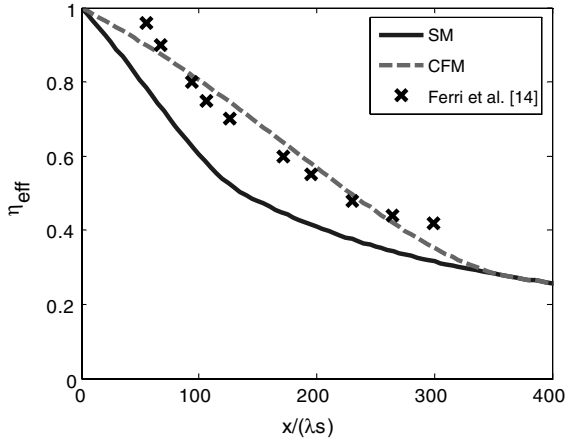

Fig. 4 Plot of film-cooling effectiveness η_{eff} as a function of nondimensional streamwise distance $x/(\lambda s)$ for a turbulent core-driven film at $\theta_0 = 0.58$ and $M_c = 0.31$ as predicted by the CFM and SM.

C. Explanation of Compressibility Effects

To understand why compressibility affects film-cooling performance, we would like to consider the effects of convective and flow Mach number (i.e., velocity or convective compressibility) as well as total temperature ratio (i.e., temperature or thermal compressibility) separately. However, this is complicated by the fact that film-cooling performance varies with downstream distance. The strategy used here is to compute the maximum value of the ratio of the compressible-to-incompressible film-cooling effectiveness (which we will refer to as the nondimensional film-cooling effectiveness) as a function of convective Mach number and total temperature ratio. The results are presented below.

1. Effect of Velocity Compressibility

Figure 6 shows peak nondimensional film-cooling effectiveness ($\eta_{\mathrm{eff(comp)}}/\eta_{\mathrm{eff(inc)}}$) and nondimensional impingement length ($x_{1,\mathrm{comp}}/x_{1,\mathrm{inc}}$) as a function of the convective Mach number for three different total temperature ratios: $\theta_0 = 1.00$, $\theta_0 = 0.50$, and $\theta_0 = 0.25$. The figure shows that increasing the compressibility (by increasing M_c) increases effectiveness by pushing the impingement point further downstream, thereby increasing the length of the protected area. Similarly, decreasing the total temperature of the coolant stream or increasing the total temperature of the core flow (i.e., driving θ_0 farther less than 1) also moves the impingement point downstream, leading to improved film-cooling effectiveness. For the case in which $\theta_0 = 1$, it is important to note that $\eta_{\mathrm{eff(comp)}}/\eta_{\mathrm{eff(inc)}}$ and $x_{1,\mathrm{comp}}/x_{1,\mathrm{inc}}$ do not equal the expected incompressible value of 1, because there are still density variations across the layer associated with the different coolant and mainstream flow Mach numbers. These are varied between Mach 0.4 and 5.5 to achieve the range of convective Mach numbers shown in the figure. This highlights the influence of the high-speed-stream flow Mach number M_{HS} on the overall velocity compressibility of a film-cooling flow.

The reasons why the nondimensional impingement length increases with increasing convective and flow Mach number and decreasing total temperature ratio can be inferred from Fig. 7. Figure 7a

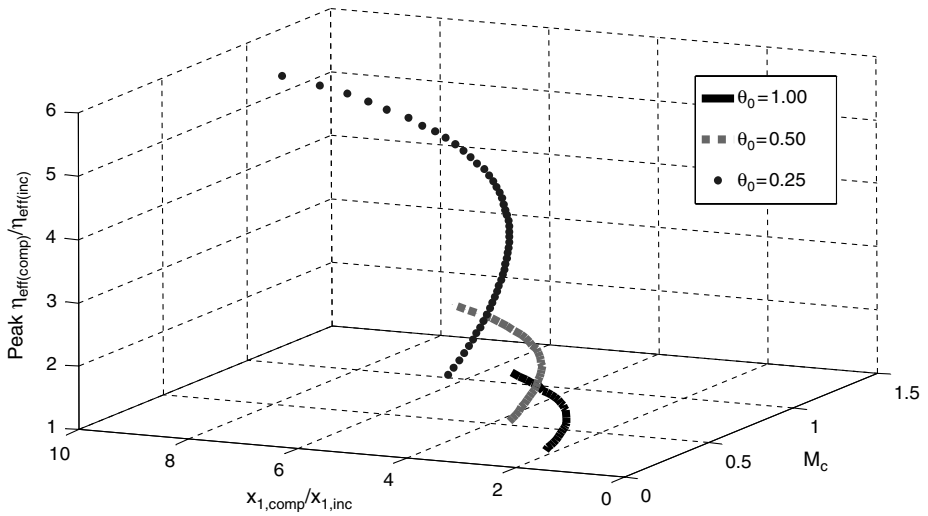

Fig. 6 Compressible (CFM) to incompressible (SM) film-cooling effectiveness (peak $\eta_{\text{eff(comp)}}/\eta_{\text{eff(inc)}}$) as a function of convective Mach number M_c and nondimensional shear-layer impingement length $x_{1,\text{comp}}/x_{1,\text{inc}}$ for a turbulent core-driven film at fixed total temperature ratios $\theta_0 = 1.00$, 0.50, and 0.25.

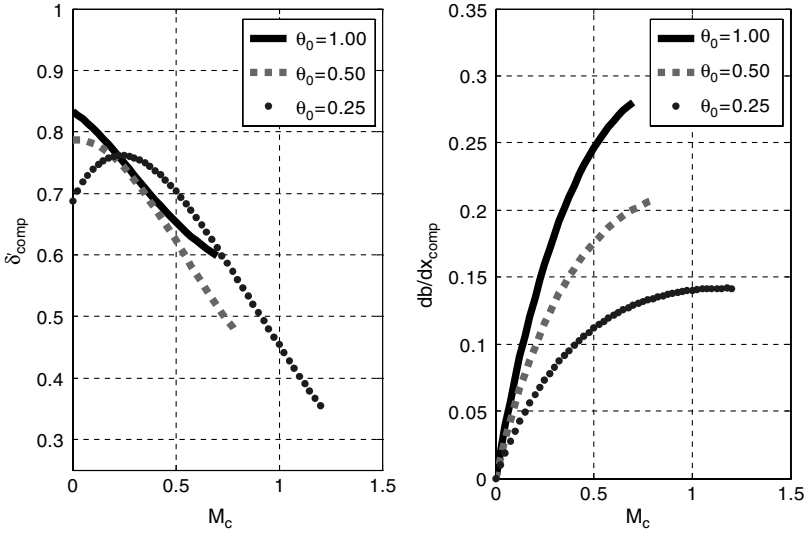

Fig. 7 Compressible shear-layer growth rate: a) normalized (δ'_{comp}) and b) unnormalized ($\mathrm{d}b/\mathrm{d}x_{\text{comp}}$) as a function of convective Mach number M_c for a turbulent core-driven film at fixed total temperature ratios, $\theta_0 = 1.00$, 0.50, and 0.25.

shows the normalized compressible shear-layer growth rate δ'_{comp} as a function of convective Mach number M_c for the same conditions explored in Fig. 6. Here, the normalized growth rate is computed by dividing the compressible growth rate defined in Eq. (19) by the incompressible growth rate, which is computed by setting $\bar{S} = 1$, in Eq. (19). Figure 7a shows that increasing M_c decreases the normalized shear-layer growth rate for most values of θ_o: a well-established finding in compressible shear-layer theory and experiments [33–35].

Figure 7b shows the variation of unnormalized compressible shear-layer growth rate $\mathrm{d}b/\mathrm{d}x_{\text{comp}}$ with convective Mach number M_c. Decreasing the total temperature ratio decreases the compressible growth rate, thereby indicating that the shear layer is thinning. This is why the nondimensional impingement length increases as θ_0 is decreased from 1.00 to 0.25. The $\theta_o = 0.25$ curve shows that for $M_c < 0.25$, increasing M_c actually increases the nondimensional growth rate. This corresponds to a situation in which $M_s > M_\infty$. However, it has a negligible impact on film-cooling effectiveness, because the unnormalized shear-layer growth rate is relatively small in this region. Taken together, these results suggest that both thermal and velocity compressibility enhance film-cooling effectiveness and do so via the same mechanism: thinning of the shear layer formed at the coolant/hot-gas-stream interface.

2. *Effect of Thermal Compressibility*

Figure 8 shows peak nondimensional film-cooling effectiveness ($\eta_{\text{eff(comp)}}/\eta_{\text{eff(inc)}}$) and nondimensional impingement distance ($x_{1,\text{comp}}/x_{1,\text{inc}}$) as a function of the total temperature ratio for three different convective Mach numbers: $M_c = 0.00$, $M_c = 0.25$, and $M_c = 0.50$. Increasing the compressibility (by decreasing θ_0) increases effectiveness by thinning the shear layer, which causes the impingement point to move downstream. Similarly, increasing the convective Mach number moves the impingement point downstream, leading to improved film-cooling effectiveness. Figure 8 tells essentially the same story as Fig. 6, except that M_c is held fixed and the total temperature is varied.

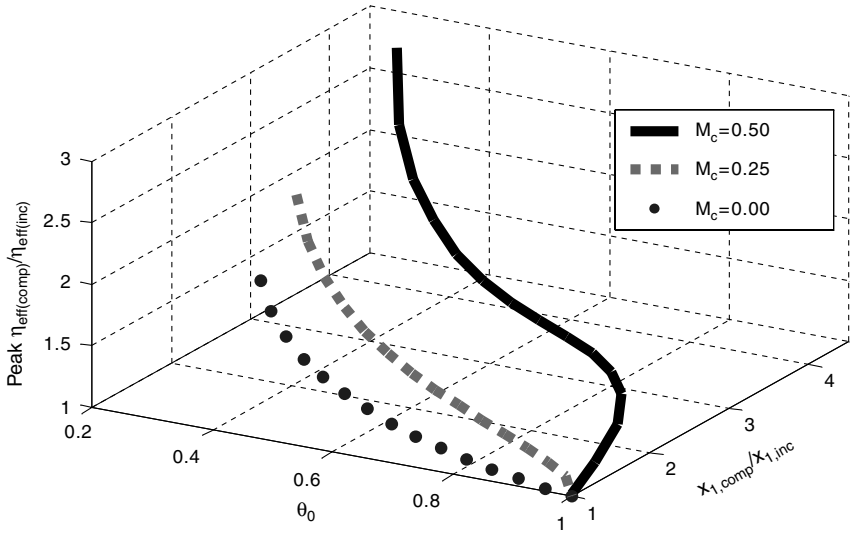

Fig. 8 Plot of peak nondimensional film-cooling effectiveness $\eta_{\mathbf{eff(comp)}}/\eta_{\mathbf{eff(inc)}}$ as a function of total temperature ratio θ_0 and nondimensional shear-layer impingement length $x_{1,\mathbf{comp}}/x_{1,\mathbf{inc}}$ for a turbulent core-driven film at fixed convective Mach numbers $M_c = 0.50, 0.25$ and 0.00 as predicted by the CFM and SM.

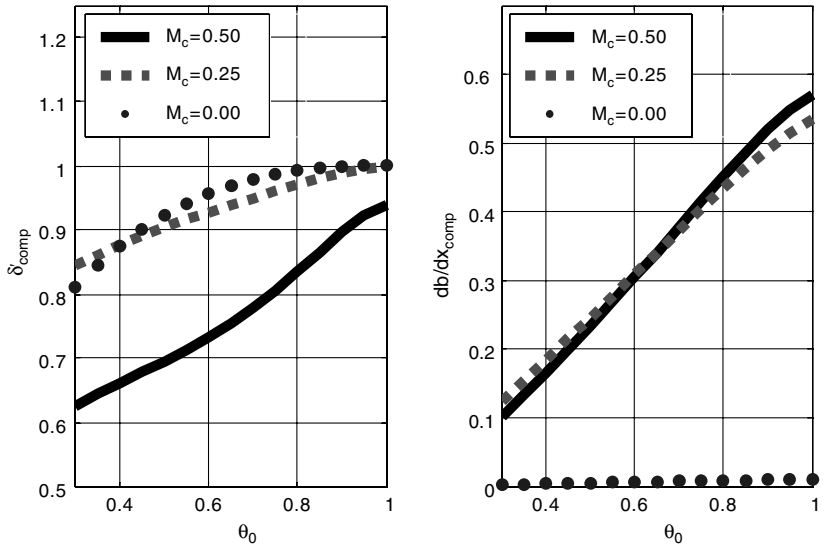

a) **b)**

Fig. 9 Compressible shear-layer growth rate: a) normalized ($\delta'_{\mathbf{comp}}$), and b) unnormalized ($\mathrm{d}b/\mathrm{d}x_{\mathbf{comp}}$) as a function of total temperature ratio θ_0 for a turbulent core-driven film at fixed total temperature ratios; $M_c = 0.50, 0.25$, and 0.00.

The explanation of Fig. 8 is also analogous to that of Fig. 6. Figure 9a shows the normalized compressible shear-layer growth rate δ'_{comp} as a function of total temperature ratio θ_0 for the same conditions explored in Fig. 8. As before, the increase in nondimensional impingement length with decreasing total temperature ratio is associated with a decrease in the normalized compressible shear-layer growth rate. Figure 9a also shows that lower total temperature ratios are required to realize compressibility effects when the convective Mach number is low. This is even more apparent in the unnormalized growth rates illustrated in Fig. 9b. Taken together, this explains why the nondimensional effectiveness is maximum at the lowest total temperature ratio and at the highest convective Mach number.

D. Use of Compressible Film-Cooling Model to Reconcile Anomalies Present in Literature

One major challenge in evaluating the importance of compressibility to film-cooling performance is reconciling the apparent contradictions in the literature mentioned in the introduction. To recap, Repukhov [4] predicts that compressibility can be ignored over a wide range of velocity and temperature conditions, whereas Hansmann et al. [4] predict that it can have a significant effect. Which is correct? The CFM model shows that both are in fact right. The reason for this is that the data Repukhov used to validate his theoretical predictions, despite being associated with a fairly low total temperature ratio ($\theta_0 < 0.4$), were taken at convective Mach numbers close to zero, and at flow Mach numbers, $M < 0.4$, where the CFM shows that compressibility effects are weak. In contrast, Hansmann et al. [5] conducted experiments at convective Mach numbers in the range $0.3 < M_c < 1.0$, with flow Mach numbers in the range $0.1 < M < 1.0$, and at very low total temperature ratios ($\theta_0 < 0.2$) in which the CFM model predicts compressibility to play a stronger role. This is illustrated below in Table 2, which compares Repukhov's [4] and Hansmann et al.'s [5] experimental conditions and the respective peak nondimensional film-cooling effectiveness, predicted using the incompressible and the compressible models.

Table 2 Summary of experimental conditions used in various film-cooling studies [4,5,17,18]

M_s	M_∞	θ_0	R	S	M_c	Peak $\eta_{\text{eff(comp)}}/\eta_{\text{eff(inc)}}$
Repukhov [4], *weak–moderate regime*						
0.38	0.23	0.36	0.99	2.86	0.001	1.52[a]
0.40	0.22	0.34	0.96	3.04	0.006	1.55[a]
Hansmann et al. [5], *strong regime*						
0.10	0.92	0.13	23.81	6.45	0.63	3.80
0.05	0.45	0.15	22.72	6.59	0.31	3.30
0.10	0.90	0.13	24.39	6.58	0.62	3.89
Cruz et al. [18], *weak regime*						
0.06	0.05	0.66	1.16	1.52	0.004	1.12
0.03	0.06	0.66	2.30	1.52	0.018	1.29
0.09	0.05	0.71	0.63	1.41	0.015	1.09
Cary and Hefner [17], *strong regime*						
1.00	6.00	0.62	2.92	0.24	1.29	1.84
1.00	6.00	0.47	3.35	0.31	1.51	3.28
1.00	6.00	0.34	3.94	0.43	1.77	5.33

[a]Since no turbulence information is available, I_v is assumed to be equal to the value used in Hansmann et al. [5] of 5.0%.

Data from other studies in which compressibility is strong (Cary et al. [17]) and weak (Cruz et al. [18]) are also included for comparison.

VI. Conclusions

The influence of compressibility on film-cooling effectiveness has been explored by extending Simon's [16] incompressible wall-jet film-cooling model to account for the effects of convective and thermal compressibility. Comparisons with experimental data show that the new model is capable of predicting film-cooling performance in three different flow regimes: weakly compressible (M_c, $M_{\text{HS}} \leq 0.3$, and $0.6 \leq \theta_0 \leq 1$), moderately compressible ($0.3 < M_c$, $M_{\text{HS}} \leq 1.0$, and $0.30 \leq \theta_0 < 0.60$), and highly compressible (M_c, $M_{\text{HS}} > 1.0$, and $\theta_0 < 0.3$). The model shows that compressibility influences film-cooling performance by changing the growth rate of the shear layer between the hot-gas and coolant streams. In general, increasing the velocity difference (by increasing M_c) and the temperature difference (by decreasing θ_0) between the main flow and the cooling film decreases the growth rate of the shear layer, moves the wall/shear-layer impingement point farther downstream, and therefore leads to an increase in film-cooling effectiveness, because more of the wall is protected. The model also resolves disagreements in the literature over whether or not compressibility is important in film-cooling problems: Compressibility effects can be important, if the convective and flow Mach numbers are high enough (greater than 0.3) and the total temperature ratio is low enough (less than 0.6).

Acknowledgments

This work has been sponsored by the Space Vehicles Technology Institute, grant NCC3-989, one of the NASA University Institutes, with joint sponsorship from the U.S. Department of Defense. Appreciation is expressed to Claudia Meyer of the NASA John H. Glenn Research Center at Lewis Field, program manager of the University Institute activity, and to John Schmisseur and Walter Jones of the U.S. Air Force Office of Scientific Research.

References

[1] Metzger, D., "Cooling Techniques for Gas Turbine Airfoils—A Survey," AGARD CPP-391, Neuilly-sur-Seine, France, 1985.

[2] Volchkov, E., Kutateladze, S., and Leontev, A., "Effect of Compressibility and Nonisothermicity on the Efficiency of Film Cooling in a Turbulent Boundary Layer," *Journal of Applied Mechanics and Technical Physics*, Vol. 7, No. 4, 1966, pp. 93–94. doi:10.1007/BF00917670

[3] Durgin, F. H., "An Insulating Boundary Layer Experiment," Ph.D. Thesis, Massachusetts Inst. of Technology, Cambridge, MA, 1957.

[4] Repukhov, V., "Effects of Compressibility and Nonisothermal Conditions on the Performance of Film Cooling," *Journal of Engineering Physics and Thermophysics*, Vol. 19, No. 5, 1970, pp. 1401–1408. doi:10.1007/BF00833476

[5] Hansmann, T., Wilhelmi, H., and Bohn, D., "An Experimental Investigation of the Film-Cooling Process at High Temperatures and Velocities," 5th AIAA/DGLR International Aerospace Planes and Hypersonics Technologies Conference, AIAA Paper 93-5062, Munich, 1993.

[6] Pedersen, D., Eckert, E., and Goldstein, R., "Film Cooling with Large Density Differences between the Mainstream and the Secondary Fluid Measured by the Heat-Mass Transfer Analogy," *Journal of Heat Transfer*, Vol. 99, 1977, pp. 620–627.

[7] Stalder, J., and Inouye, Mamoru, "A Method of Reducing Heat Transfer to Blunt Bodies by Air Injection," NACA RMA56B27a, 1956.

[8] Ferri, A., and Libby, P., "The Use of Helium for Cooling Nozzles Exposed to High Temperature Gas Streams," WADC TN 55-318, Mar. 1956.

[9] Danneberg, R., "Helium Film Cooling of a Hemisphere at a Mach Number of 10," NASA TN-D 1550, Nov. 1962.

[10] Goldstein, R., Eckert, E., Tsou, F., and Haji-Sheikh, A., "Film Cooling with Air and Helium Injection through a Rearward-Facing Slot into a Supersonic Air Flow," *AIAA Journal*, Vol. 4, No. 6, 1966, pp. 981–985. doi:10.2514/3.3591

[11] Parthasarathy, K., and Zakkay, V., "An Experimental Investigation of Turbulent Slot Injection at Mach 6," *AIAA Journal*, Vol. 8, No. 7, 1970, pp. 1302–1307. doi:10.2514/3.5889

[12] Kanda, T., Masuya, G., Ono, F., and Wakamatsu, Y., "Effect of Film Cooling/Regenerative Cooling on Scramjet Engine Performances," *Journal of Propulsion and Power*, Vol. 10, No. 5, 1994, pp. 618–624. doi:10.2514/3.23771

[13] Schuchkin, V., Osipov, M., Shyy, W., and Thakur, S., "Mixing and Film Cooling in Supersonic Duct Flows," *International Journal of Heat and Mass Transfer*, Vol. 45, No. 22, 2002, pp. 4451–4461. doi:10.1016/S0017-9310(02)00151-5

[14] Ferri, A., Mahrer, A., and Hefner, J., "Investigation of Slot Cooling at High Subsonic Speeds," *AIAA Journal*, Vol. 14, No. 7, 1976, pp. 880–885. doi:10.2514/3.7163

[15] Cary, A., and Hefner, J., "Film-Cooling Effectiveness and Skin Friction in Hypersonic Turbulent Flow," *AIAA Journal*, Vol. 10, No. 9, 1972, pp. 1188–1192. doi:10.2514/3.50348

[16] Simon, F. F., "Jet Model for Slot Film Cooling with Effect of Free-Stream and Coolant Turbulence," NASA TP-2655, 1986.

[17] Cary, A., and Hefner, J., "Film-Cooling Effectiveness and Skin Friction in Hypersonic Turbulent Flow," *AIAA Journal*, Vol. 10, No. 9, 1972, pp. 1188–1192. doi:10.2514/3.50348

[18] Cruz, C., Raffan, F., Cadou, C., and Marshall, A., "Characterizing Slot Film Cooling Through Detailed Experiments," International Mechanical Engineering Conference & Exposition, Chicago, ASME International, Paper 15899, Nov. 2006.

[19] Sturgess, G., and Pfeifer, G., "Design of Combustor Cooling Slots for High Film Effectiveness. Part II—Film Initial Region," *Journal of Engineering for Gas Turbines and Power*, Vol. 108, No. 2, 1986, pp. 361–369. doi:10.1115/1.3239912

[20] Goldstein, R., "Film Cooling," *Advances in Heat Transfer*, Vol. 7, 1971, pp. 321–379. doi:10.1016/S0065-2717(08)70020-0

[21] Cary, A., and Hefner, J., "Film Cooling Effectiveness in Hypersonic Turbulent Flow," *AIAA Journal*, Vol. 8, No. 11, 1970, pp. 2090–2091. doi:10.2514/3.6062

[22] Stollery, J., and El-Ehwany, A., "A Note on the Use of a Boundary-Layer Model to Correlate Film-Cooling Data," *International Journal of Heat and Mass Transfer*, Vol. 8, No. 1, 1965, pp. 55–65. doi:10.1016/0017-9310(65)90097-9

[23] Juhasz, A., and Marek, C., "Combustor Liner Film Cooling in the Presence of High Free Stream Turbulence," NASA TN D-6360, 1971.

[24] Abramovich, G., *The Theory of Turbulent Jets*, MIT Press, Cambridge, MA, 1963, pp. 163–305.

[25] Yakovlevskiy, O., "The Problem of the Thickness of the Turbulent Mixing Zone between Two Gas Streams of Different Velocity and Density," *Izvestiya Akademiya Nauk USSR. Otdeleniye Tekhnicheskikh Nauk*, Vol. 10, 1958, pp. 153–155.

[26] Ko, S., and Liu, D., "Experimental Investigation on Effectiveness, Heat Transfer Coefficient, and Turbulence of Film Cooling," *AIAA Journal*, Vol. 18, No. 8, 1980, pp. 907–913. doi:10.2514/3.50833

[27] Anderson, J., *Modern Compressible Flow*, 3rd ed., McGraw–Hill, New York, 2003.

[28] Schlichting, H., *Boundary Layer Theory*, 4th ed., McGraw–Hill, New York, 1960.
[29] Abramowitz, M, and Stegun, I., *Handbook of Mathematical Functions*, Dover, New York, 1972, p. 887.
[30] Stoer, J., and Bulirsch, R., *Introduction to Numerical Analysis*, Springer, New York, 2002, pp. 171–181.
[31] Dellimore, K., Cruz, C., Marshall, A., and Cadou, C., "Influence of a Streamwise Pressure Gradient on Film Cooling Effectiveness," *Journal of Thermophysics and Heat Transfer*, Vol. 23, No. 1, 2009, pp. 120–128.
doi:10.2514/1.35717
[32] Lushchik, V., and Yakubenko, A., "Tangential-Slot Film Cooling on a Plate in Supersonic Flow. Comparison of Calculation and Experiment," *Fluid Dynamics*, Vol. 36, No. 6, 2001, pp. 926–933.
doi:10.1023/A:1017914710250
[33] Papamoschou, D., and Roshko, A., "The Compressible Turbulent Shear Layer: An Experimental Study," *Journal of Fluid Mechanics*, Vol. 197, No. -1, 1988, pp. 453–477.
doi:10.1017/S0022112088003325
[34] Papamoschou, D., "Experimental Investigation of Heterogeneous Compressible Shear Layers," Ph.D. Dissertation, California Inst. of Technology, Pasadena, CA, 1986.
[35] Papamoschou, D., and Roshko, A., "Observations of Supersonic Free Shear Layers," *Indian Academy of Sciences*, Vol. 12, No. 1, 1988, pp. 1–14.
doi:10.1007/BF02745657